UV–vis versus visible degradation of Acid Orange II in a coupled CdS/TiO$_2$ semiconductors suspension

Y. Bessekhouad [a,b], N. Chaoui [b], M. Trzpit [b], N. Ghazzal [b], D. Robert [b,*], J.V. Weber [b]

[a] *Ecole Nationale Vétérinaire, LSVER, BP 161-El Harrach, Alger, Algeria*
[b] *Laboratoire de Chimie et Applications (LCA)-Université Paul Verlaine-Metz, Rue Victor Demange, 57500 Saint-Avold, France*

Abstract

TiO$_2$, CdS and coupled CdS/TiO$_2$ powders with CdS percentage varied from 5 to 50% (w/w) have been prepared by a sol–gel method. These pure and composite semiconductors were tested for the photocatalytic degradation of an anionic azo-dye, i.e. Orange II in aerated aqueous suspension under UV–vis and visible ($\lambda > 400$ nm) illumination. The photocatalytic efficiency of the CdS/TiO$_2$ couples is found to strongly depend on the proportion of CdS. Under UV–vis light, CdS/TiO$_2$ couples containing a low proportion of CdS are found to be as efficient as pure TiO$_2$ which shows the best photocatalytic activity. Under visible illumination, these formers exhibit faster degradation rate than both isolated components of the composite photocatalyst. The results obtained under both illumination conditions are compared and discussed in order to elucidate the respective role of Acid Orange II and CdS in the photosensitization mechanism of TiO$_2$.
© 2006 Elsevier B.V. All rights reserved.

Keywords: Photosensitization; Orange II; Cadmium sulphide; Titanium dioxide

1. Introduction

During the recent 10 years, the use of TiO$_2$ nanoparticules for the degradation of organic pollutant in water has received extensive attention. TiO$_2$ is an excellent photocatalyst that can mineralizes a large range of organic pollutants even among the most refractory ones including pesticides [1,2], herbicides [3,4] and dyes [5,6]. However, it is a large gap semiconductor ($E_g = 3.2$ eV) that can only be excited by UV radiation with wavelength below 380 nm. Practically, this factor strongly limits the use of solar spectra as a source for the photoreaction. In some cases, the substrate, most often a dye, can help for the extent of the absorption spectra of TiO$_2$ in the visible. In such a process, the dye molecule is excited by visible light to a suitable energy level followed by electron transfer to the conduction band of TiO$_2$. The dye is converted in an ion radical and the electron is scavenged by adsorbed molecular oxygen to form radicals (O$_2^{\bullet-}$, OH$^\bullet$ and HO$_2^\bullet$) that degrade the dye. This process, referred as photo-sensitization, has been the subject of numerous publications [5,6].

Another major limiting factor is the high rate of recombination of the photogenerated electron/hole pairs. It results in a poor rate of electrons (and holes) that reaches the interface semiconductor/liquid where the redox reactions inherent to photocatalyzed degradation take place. A possible way out consists in coupling a large band gap semiconductor with a smaller band gap semiconductor presenting suitable potential energies [7,8]. For example, in CdS/TiO$_2$ the photogenerated electrons in CdS are transferred into the TiO$_2$ particles while the holes remain in the CdS particle. This not only helps for charge separation by isolating electrons and holes in two distinct particles but at the same time, allows the extension of the photoresponse of the photocatalyst in the visible. In the mid 1990s, Serpone et al. [7] reported for the first time the photocatalyzed oxidation of several phenol-based molecules by coupled semiconductors suspension in which the beneficial effect of the charge transfer was clearly demonstrated. In addition to the flat band potential of the components, the photocatalytic performance of the coupled semiconductors is also related to the geometry of the particles, the surface contact between particles and the particles size [7]. These parameters strongly depends on the manner the

* Corresponding author.
  E-mail address: drobert@iut.univ-metz.fr (D. Robert).

couples are prepared. We demonstrated recently the influence of the coupling method on the photocatalytic activity by comparing the photocatalytic activity of couples prepared by precipitating CdS on TiO_2 to those obtained by a simple mixture of the components [8].

However, the use of CdS as a photocatalyst has been limited due to its anodic decomposition, i.e. photocorrosion [7,9]. It is a well known fact that from a practical point of view, the use of CdS in coupled system is not recommendable owing to the release of toxic cadmium [7,9]. However, from a fundamental point of view, there are still some attractive mechanistic aspects that are worth to be examined, especially when it deals with dye degradation. We put emphasis on the fact that improving the photoactivity of TiO_2 *for practical application* is beyond the scope of this report.

In this study, CdS/TiO_2 couples have been prepared by a sol–gel method *by precipitating TiO_2 on CdS* in order: (i) to exploit the maximum optical absorption properties of CdS in the visible and (ii) to increase the surface contact between CdS and TiO_2 particules. A balance between the photosensitization and the UV–vis filtering of CdS is searched by varying the amount of CdS in the couple in a range 5–50% of the total weight of the couple. The photodegradation Orange II in aerated condition carried out under UV–vis and visible illumination serves as a reference test for the evaluation of the photocatalytic activity of the pure and composites semiconductors. The evidence for the charge transfer process is evidenced by comparing the photocatalytic activities of isolated components, both in visible and UV–vis illumination, to those of the composite semiconductors. The contribution of the dye sensitization of TiO_2 to the overall photocatalytic mechanism of TiO_2 is also examined. Finally, the amount of Cd^{2+} in the solution after illumination of the solution containing the prepared material is compared to that containing a physical mixture of the constituents.

2. Experimental

2.1. Materials

All of the reagents used in this work were of analytical grade and were used without any further purification: $Cd(NO_3)_2$ (Aldrich), thiourea $SC(NH_2)_2$ (Aldrich), tetraisopropylorthotitanate $Ti(OC_3H_7)_4$ (Aldrich, 97%), ethanol (SdS-France, 99.9%), methanol (SdS-France, 99.9%) and Orange II (Sigma Chemical Co.).

2.2. Semiconductors preparation

2.2.1. Preparation of the pure photocatalysts

Prior the preparation of the couples, pure semiconductors were prepared. CdS nanoparticules were prepared by direct reactions between $Cd(NO_3)_2$ salt and thiourea in an ammonia bath (NH_4OH, 14.4 M) at 85 °C for 1 h. The orange–red precipitate was subsequently washed with acetone, water and absolute ethanol and then dried at 110 °C overnight. The powder was heat-treated at 450 °C for 2 h with a heating rate of 3 °C/min. After cooling, the powder was dispersed in acetic acid solutions

at pH ∼4.5 for 30 min. The sample was recovered by filtration, and washed several times with distilled water before being dried at 110 °C overnight. Pure CdS is then obtained after heating at 350 °C for 1 h.

TiO_2 was prepared by dissolving $Ti(OC_3H_7)_4$ in methanol/ethanol solution with molar ratio 1:1:10. The obtained solution was maintained at 75 °C for 3 h and an appropriate amount of water was added dropwise into the hot solution (75 °C). After gelling, the sample was dried at 110 °C overnight and then heat-treated in air for 2 h at 450 °C with a heating rate of 3 °C/min.

2.2.2. Preparation of composite photocatalysts

The described preparation procedure used to obtain pure TiO_2 was used for the preparation of the coupled semiconductors, except that an appropriate amount of CdS was dispersed in alcohol solution and sonicated (30 min) before adding $Ti(OC_3H_7)_4$. The amount of CdS was varied from 5 to 50% (w/w). The couple were dried at 110 °C overnight and then heat-treated in air for 2 h at 450 °C with a heating rate of 3 °C/min.

2.3. X-ray diffraction (XRD)

X-ray diffraction patterns were collected at 295 K using Cu Kα ($\lambda = 0.15418$ nm) radiation. Structural assignments were made in reference to the JCPDS powder diffraction files. The average crystalline sizes of each phase were determined from the Scherrer equation using the full-width at half-maximum (FWHM) of the peak presenting the highest intensity and taking into account the instrument broadening.

2.4. UV–vis diffuse reflectance spectroscopy

Diffuse reflectance spectra of pure and composite semiconductor were recorded by means of a UV–vis spectrophotometer (Perkin-Elmer) equipped with an integrating sphere. A $BaSO_4$ pellet was used as a reference. The spectra were recorded at room temperature in the spectral range 200–800 nm.

2.5. Scanning electron microscopy (SEM)

Scanning electron microscopy observations were performed by means of a HITACHI S2500 instrument in both secondary and backscattered electrons modes.

2.6. Measurement of photocatalytic activity

Solar box ATLAS Suntest *CPS*+ simulating natural radiation and equipped with a Xenon lamp (250 W) was used. Photocatalytic experiments were performed under UV–vis light or under visible light. In that latter case, a PMMA sheet (poly(methyl methacrylate)) with a thickness of 12 mm was used as an optical filter to cut the UV radiation below 390 nm. Acid Orange II (OII, hereafter), an anionic dye was used as a model pollutant for the degradation. Its molecular structure is displayed in Fig. 1, together with its UV–vis absorption spectrum in water
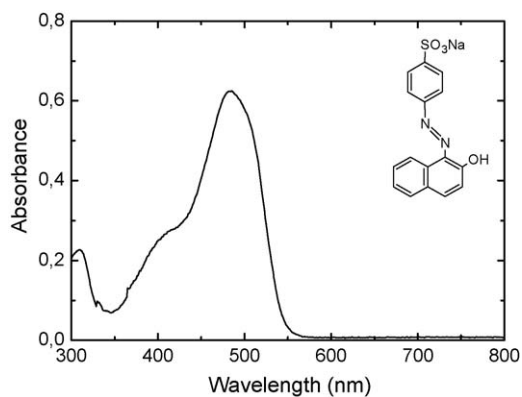
Fig. 1. UV–vis absorption spectra and molecular structure of Orange II.

at natural (pH 5.8). Pure semiconductors and couples were dispersed in a volume of 100 ml of dye (10 mg/l) solution. The weight of pure semiconductor used for photocatalytic tests was 50 mg (0.5 g/l) keeping the amount of TiO_2 for each couple to 50 mg. Before each irradiation, the mixtures were sonicated during 5 min in order to disperse the catalysts and the solutions were maintained in the dark during 1 h in order to reach the adsorption equilibrium. During the photocatalytic test, 5 ml of the solution was taken out at given irradiation time intervals and analyzed by UV–vis spectrophotometer (Shimadzu). The measurement of maximum absorbance was taken for Orange II was 485 nm.

2.7. Adsorption

The OII adsorption on TiO_2 and CdS in aqueous solution was determined by stirring during 2 h in the dark 50 cm^3 of the dye solution at an initial concentration of 10 mg/l with a fixed weight of 25 mg of photocatalyst. The suspension was then filtered by centrifugation. The absorbance of the filtrate was measured to determine the equilibrium concentration C_e and the concentration decrease $\Delta C = C_i - C_e$ used to determine the percentage of adsorbed catalyst.

2.8. Cadmium release measurement

The photocorrosion of CdS has been evaluated for the couples by measuring the Cd^{2+} concentration in the solution after 35 min under visible illumination. These measurements have been performed by means of atomic absorption spectrometry (Unicam 939).

3. Results

3.1. Structure analysis

Fig. 2 shows the XRD pattern of the synthesized TiO_2, CdS and the CdS/TiO_2 couples with 5 and 50% (w/w) of CdS. The pure CdS powder (Fig. 2a) can be well assigned to pure hexagonal phase (JCPDS no. 41-1049) with a crystallite size of about 40 nm estimated from the FWHM of the (1 0 1) peak. For pure TiO_2 (Fig. 2b), the pattern agrees with anatase structure (JCPDS file no. 21-1272) with trace of brookite (JCPDS no. 29-1360).
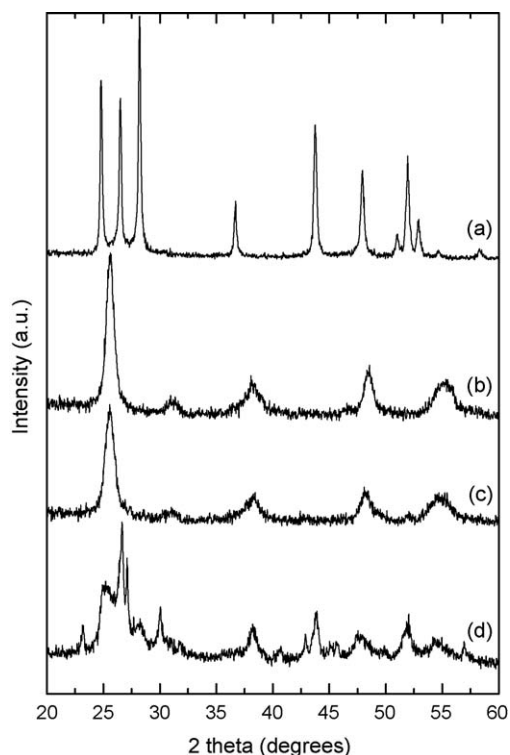

Fig. 2. XRD patterns of the synthesized pure and composite powders: (a) TiO_2, (b) CdS, (c) CdS(5%)/TiO_2 and (d) CdS(50%)/TiO_2.

The size of the anatase crystallites was estimated to be 9 nm. At low concentration (5%; Fig. 2c), the presence of CdS has no significant effect on the TiO_2 crystalline structure observed for the pure powder. By contrast, when the CdS amount is increased (50%; Fig. 2d), the structure of TiO_2 shows significant changes. Peaks attributed to rutile and other non identified are observed in addition to those of anatase, brookite and the hexagonal phase of CdS.

The SEM micrograph in backscattered electrons mode of the CdS(5%)/TiO_2 couple is presented in Fig. 3. The micrograph shows agglomerates with irregular morphology and size ranging from few micrometer down to hundreds of nanometer. The compositional contrast, inherent in backscattered electron micrographs, shows the distribution of CdS-rich region (in bright) into the TiO_2 particles (in dark grey). Both grey and bright regions on the micrograph have been analyzed at the limit of resolution for the EDS system. The basic fact that the titanium is detected in the dark region and Cd in the light region confirms the assumption made from the examination backscattered electron micrographs. However, traces of Cd are also detected in dark regions suggesting that a part of the nanosized CdS particles coexist within a titanium oxide matrix.

3.2. UV–vis diffuse reflectance spectroscopy

Fig. 4 shows the UV–vis absorption spectra of pure CdS and TiO_2 and coupled CdS(x%)/TiO_2 for several amounts of CdS ranging from $x = 10$ to 50%. The absorption edge of pure TiO_2 (Fig. 4a) is observed at about 400 nm whereas that of pure CdS (Fig. 4e) is at about 580 nm. Compared to pure TiO_2,
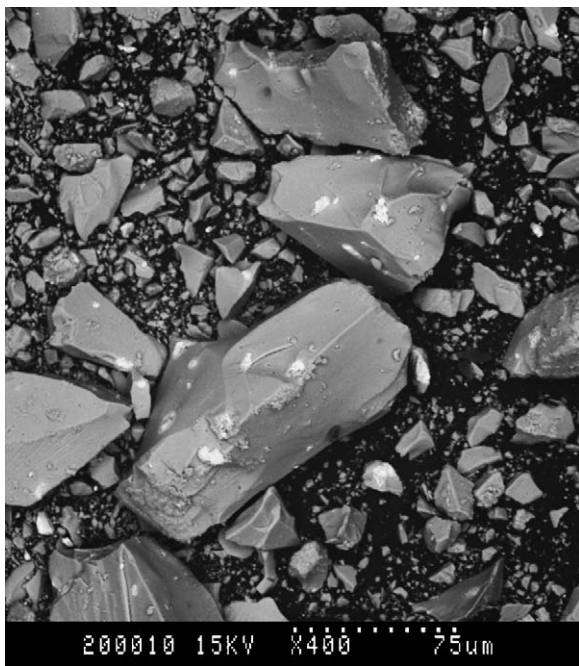
Fig. 3. Scanning electron micrographs in backscattered electrons mode of CdS(5%)/TiO$_2$ composite semiconductor.

the couples CdS(x%)/TiO$_2$ show an absorption plateau in the region 400–580 nm corresponding to the contribution of CdS to the absorption spectra. The level of the plateau increases with increasing CdS concentration. These results show that the coupled semiconductor can be excited by visible light. The colour of powder containing low amount of CdS is yellow and turn to orange when the amount of CdS is increased.

3.3. Degradation of Orange II

Fig. 5 shows the concentration decrease of Orange II in TiO$_2$, CdS and CdS(x%)/TiO$_2$ (with x = 5, 10, 30 and 50) couples suspension, under UV–vis (A) and visible (B) illumination. Table 1 presents the degradation rates as function of CdS content in the couples. Prior to these experiments, we carried out a photolysis on Orange II which did not reveal any detectable concentration change of OII. Therefore, any change in the concentration
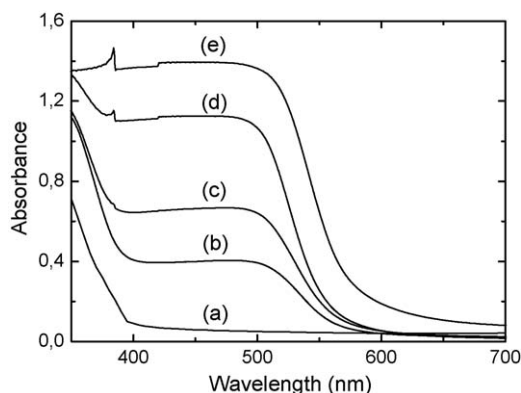

Fig. 4. UV–vis absorbance spectra of the pure and composite semiconductors: (a) TiO$_2$, (b) CdS(10%)/TiO$_2$, (c) CdS(30%)/TiO$_2$, (d) CdS(50%)/TiO$_2$ and (e) CdS.

of Orange II can be related to heterogeneous photocatalytic reaction. Whatever the nature of the suspension, the photodegradation of OII shows apparent first order kinetic.

Under UV–vis illumination (Fig. 5A), the degradation rates of TiO$_2$ and CdS(x%)/TiO$_2$ couples with low CdS amount (x = 5 and 10), do not present any significant difference (0.025 min^{-1}). These latter shows the best photocatalytic activity. By contrast, when the CdS amount is increased (x = 30 and 50), the degradation rate decreases by about a factor 2 (0.014 and 0.017 min^{-1}, respectively) and becomes even slower for pure CdS suspension (0.01 min^{-1}).

Under visible illumination (Fig. 5B), the time concentration evolutions show noteworthy differences with what observed under UV–vis illumination. First, the degradation rate of the TiO$_2$ suspension shrinks but, surprisingly, still shows a photocatalytic activity (0.003 min^{-1}). Because of its wideband gap (3.2 eV), it is supposed that TiO$_2$ with anatase structure can only be activated by UV light of wavelength below 380 nm. In the visible, CdS (0.01 min^{-1}) turns out to be a better photocatalyst than both TiO$_2$ and CdS-rich couples (with x = 30 and 50). But the most captivating observation is done for CdS-poor couples (x = 5 and 10) which show the fastest degradation rate. This latter is twice that of pure CdS and at least factor five that of TiO$_2$.

3.4. Release of cadmium (photocorrosion)

The photocorrosion of CdS has been evaluated by measuring the Cd^{2+} concentration in the solution after 35 min vis-
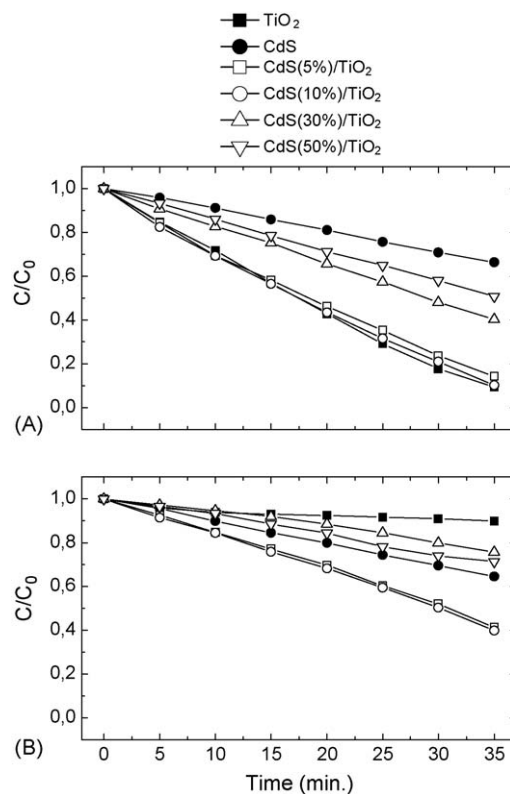

Fig. 5. Photocatalyzed degradation in aerated aqueous media of Orange II in the presence of CdS, TiO$_2$ and CdS/TiO$_2$ composite semiconductors under: (A) UV–vis and (B) visible illumination.

Table 1
Initial degradation rates of OII in CdS/TiO$_2$ suspensions with amounts of CdS ranging from 0 to 100%

	Degradation rate ($\times 10^{-3}$ min^{-1})		[Cd^{2+}]^a (mg/l)	
	UV–vis	Visible	Sol–gel	Physical mixture
TiO$_2$	25	3	–	–
CdS(5%)/TiO$_2$	25	16	13.2 ± 0.3	12.7 ± 0.3
CdS(10%)/TiO$_2$	25	16	17.1 ± 0.3	18.2 ± 0.3
CdS(30%)/TiO$_2$	17	7	–	–
CdS(50%)/TiO$_2$	14	8	–	–
CdS	10	10	–	–

^{a} Measured after 30 min under visible illumination.

ible illumination. These measurements have been performed for the two couples showing the best photocatalytic activities (CdS(5%)/TiO$_2$ and CdS(10%)/TiO$_2$) and compared to a CdS/TiO$_2$ physical mixture containing the same CdS amount. The obtained concentrations are presented in Table 1. As expected, the results show that [Cd^{2+}] increases when the CdS amount in the couple is increased. When the amount of CdS is increased by a factor 2, the Cd^{2+} release increases by about 50%. However, for a given CdS amount, there is no clear differences between the Cd^{2+} concentrations obtained with both powders showing that the way the couple is prepared has a poor influence on the stabilization of CdS.

4. Discussion

Adsorption of OII on TiO$_2$ and CdS has been measured according to the procedure described in the experimental section. When the equilibrium concentration was reached, the initial OII concentration (10 mg/l) decreased by 4% in the CdS suspension whereas no concentration change was measured in the TiO$_2$ suspension. This does not necessarily mean that there is no adsorption at all onto TiO$_2$ but rather the concentration change is below the detection limit of the apparatus used. Taking account of the accuracy of the concentrations, the calibration curve (absorbance versus concentration) used, the technical specifications of our spectrophotometer, we estimate the threshold for a significant concentration change in a $C = 10$ mg/l in OII solution to be about $\Delta C = 0.1$ mg/l, i.e. 1% of the concentration. This would mean that in the case of TiO$_2$, the adsorption, if it occurs, gives rise to a concentration decrease inferior to 1%. This assumption is consistent with the adsorption measurements of OII onto P25 TiO$_2$ reported by Kiriakidou et al. [10]. These authors showed that the adsorption of OII on TiO$_2$ strongly depends on pH and according to the measurements they performed at pH 6, as it the case in this study, for an initial concentration of 10 mg/l (i.e. 2.85×10^{-5} mol/l) the amount of OII adsorbed per gram of P25 TiO$_2$ is of the order of 1×10^{-6} mol/g or below. On the other hand, P25 TiO$_2$ presents a BET surface area of 50 m^2/g that is threefold the value of the TiO$_2$ used in this study (17 m^2/g). Since the adsorption amount decreases with decreasing BET area, we can reasonably consider that the amount adsorbed OII per gram on our material to be rather of the order of $n = 1 \times 10^{-7}$ mol/g. The molarity decrease $\Delta C = nW/V$ (with W the weight of TiO$_2$ in grams and V the volume of the dye solution) induced by the

adsorption of $n = 1 \times 10^{-7}$ mol/g is found to be 5×10^{-8} mol/l, e.g. 0.2% of the initial concentration which is far below the detection limit allowed by our experiment.
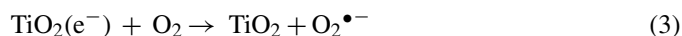
4.1. Dye sensitization

The assumption for which a low amount of OII is adsorbed on the TiO$_2$ surface is consistent with the slow degradation OII (0.003 min^{-1}) observed in TiO$_2$ suspension under visible illumination (Fig. 5B). This observation is in agreement with earlier reports on the degradation of OII in P25 TiO$_2$ suspension under visible illumination [5,6]. It is due to a sensitization mechanism [5,6]. The dye molecule when adsorbed on the photocatalyst may absorb visible light to produce a singlet and/or triplet state of OII molecule the singlet state ^{1}OII* is more reactive than the triplet.

$$^1OII_{ads} + h\nu \rightarrow {}^1OII_{ads}{}^* \tag{1}$$

If the oxidation potential of the excited state is more negative than the potential of the conduction band of TiO$_2$ particles, an electron is injected into the conduction band of TiO$_2$ from the excited state ^{1}OII$_{ads}{}^*$. The oxidation potential of the excited singlet state of OII has been reported to be -1.25 V versus NHE [10] that is more negative than the CB level of TiO$_2$ (-0.5 V versus NHE) making thermodynamically possible the electron transfer. Therefore, the dye is converted to the cationic dye radical (Eq. (2)).

$$^1OII_{ads}{}^* + TiO_2 \rightarrow {}^1OII_{ads}{}^{\bullet+} + TiO_2(e^-) \tag{2}$$
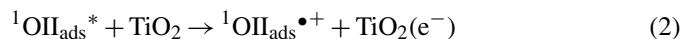
The injected electron can be then scavenged by adsorbed oxygen for producing oxygen superoxide radicals O$_2^{\bullet-}$. This radical may generate hydroxyl (OH$^\bullet$) and hydroperoxy (HO$_2^\bullet$) that can mineralize the substrate if the suspension is illuminated for several hundreds of minutes [11].

$$TiO_2(e^-) + O_2 \rightarrow TiO_2 + O_2^{\bullet-} \tag{3}$$

$$^1OII_{ads}{}^{\bullet+} \rightarrow products \tag{4}$$

$$^1OII_{ads}{}^{\bullet+} + O_2^{\bullet-} (or\ OH^\bullet\ or\ HO_2^\bullet) \rightarrow products \tag{5}$$

The huge difference between the activity of TiO$_2$ under UV–vis and that under visible illumination reveals the minor contribution of the sensitization mechanism under UV–vis light compared to the well known process of direct excitation of TiO$_2$,
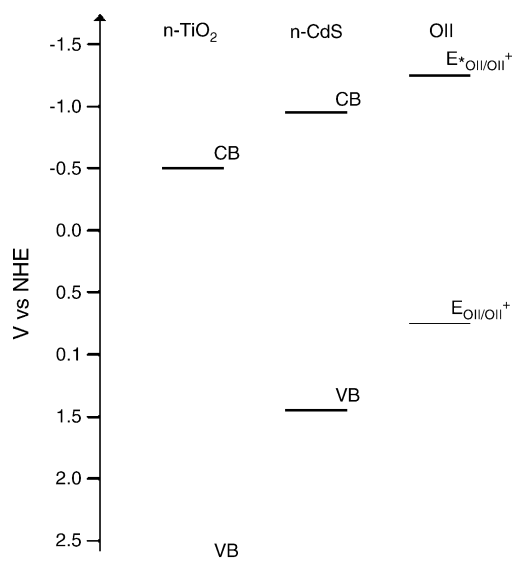
Fig. 6. Relative positions of the redox potential of TiO_2, CdS and OII.

involving both electrons and holes, by photons possessing higher energy than the band gap of TiO_2 (3.2 eV).

For the case of OII degradation in CdS suspension, no significant difference is observed between UV–vis and visible illumination. Therefore, it is difficult to assess for the contribution of the sensitization mechanism to the degradation rate. Hence, these results demonstrate that the UV part of the light (4%) has little influence on the degradation rate under UV–vis irradiation. Because of both spectral characteristics of the simulator we use and the optical response of CdS (Fig. 4), the photocatalytic process is mainly governed by visible light. Though, the dye sensitization mechanism cannot be excluded because: (i) the capacity of CdS for adsorbing OII (4% of the initial concentration of the solution) and (ii) the oxidation potential of the singlet state $^1OII^*$ (−1.25 V versus NHE) is more negative than the CB level of CdS (−0.95 V versus NHE).
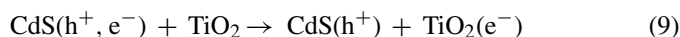
4.2. Dye and CdS sensitization

The basic thermodynamic conditions for the occurrence of interparticle charge transfer between two semiconductors are well documented [7,8,11]. Briefly, for an efficient electron transfer, the conduction band of TiO_2 (wideband gap semiconductor) must be more anodic than that of the sensitizer (narrowband gap semiconductor) and for an efficient hole transfer from TiO_2 to the sensitizer, the valence band of the sensitizer must be more cathodic than that of TiO_2. In addition to the flat band potential of the components, the photocatalytic performance of the couple is also related to the geometry of the particles, the surface contact between particles and the particles size [7]. As shown in Fig. 6, the conduction bands of TiO_2 and CdS are suitably disposed for electrons transfer may occur from the CB of CdS to that of TiO_2 when CdS is excited by visible light. It appears also from the SEM micrographs (Fig. 3) and the EDS analysis that the way we synthesize the couples leads to a rather homogeneous distribution of CdS among the TiO_2 particles. Therefore, the

intrinsic properties of the components as well as the method used for coupling the semiconductors fulfil the main conditions that allow interparticle charge transfer. The electron transfer between CdS and TiO_2 particles is clearly demonstrated in Fig. 5B. The degradation of OII in CdS(x%)/TiO_2 suspension with $x = 5$ and 10 under visible illumination is found to be six and two times faster than the isolated components, i.e. TiO_2 and CdS, respectively. This result is in good agreement with earlier work reported by Serpone et al. [7] in which the occurrence of interparticles electrons transfer in CdS/TiO_2 was verified for the oxidation of phenol-based compounds. Furthermore, the suitable positions of the redox level of the $^1OII_{ads}^*$ molecule legitimates the process of charge transfer that leads to degradation of OII. The potential difference between the redox levels of $^1OII^*$ (Eq. (1)) and the CB of CdS (see Fig. 6) as well as the capacity of CdS to adsorb OII allow charge injection into the CdS conduction band as described in the former section.

$$^1OII_{ads}^* + CdS \rightarrow {}^1OII_{ads}^{\bullet+} + CdS(e^-) \tag{6}$$
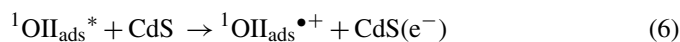
And thus, the electrons injected in the CB of CdS (Eq. (6)) and those coming from CdS direct excitation (Eq. (7)) may be transferred into the CB level of TiO_2 as described by Eqs. (8) and (9). The molecules degradation occurs according to Eqs. (3)–(5).

$$CdS + h\nu \rightarrow CdS(h^+, e^-) \tag{7}$$

$$CdS(e^-) + TiO_2 \rightarrow CdS + TiO_2(e^-) \tag{8}$$

$$CdS(h^+, e^-) + TiO_2 \rightarrow CdS(h^+) + TiO_2(e^-) \tag{9}$$

The observed slow degradation of OII in pure TiO_2 suspension under visible light strongly suggests that the mechanism described by Eqs. (6)–(9) prevails on the direct charge transfer from excited $^1OII^*$ molecule to TiO_2. As commented for pure CdS, the sensitization mechanism is thermodynamically possible but it is difficult to compare its contribution to the mechanism involving direct excitation of CdS nanoparticles.

The low efficiency of CdS-rich couples ($x = 30$ and 50% CdS) may have different reasons. It could be that with increasing amount of CdS, the contact surface between CdS particles and TiO_2 particles becomes less good. On the other hand, increasing the CdS amount could increase the mean path of the electron through the CdS particles. This could favour the recombination of the electrons with the holes generated in the CdS particles. The results shown in Fig. 5A and B also reveal that when the CdS proportion is increased, the couple tends to behave like pure CdS. In other words, above a critical CdS amount that lies between 10 and 30%, the photocatalytic process is mainly govern by CdS that show a poor photocatalytic activity.

5. Conclusion

Coupled CdS/TiO_2 with CdS percentage (w/w) varied from 5 to 50% have been prepared by precipitating TiO_2 on CdS. The photocatalytic efficiency of the CdS/TiO_2 couples strongly depends on the proportion of CdS. Under UV–vis light, CdS/TiO_2 couples containing a low proportion of CdS (5 and

10%) and pure TiO_2 show the best photocatalytic activity. Under visible illumination, these formers exhibit a faster degradation rate than both isolated components evidencing an interparticle electron transfer. The fact that the dye adsorbs much more on CdS than TiO_2 and the suitable level of its singlet excited state suggest that electron transfer from the dye to CdS contribute to the degradation mechanism. Finally, the loss of Cd^{2+} in the solution upon illumination of the sol–gel product is comparable to that of a simple mixture of both components in the same proportion.

References

[1] S. Malato, J. Blanco, C. Richter, B. Milow, M.I. Maldonado, Water Sci. Technol. 40 (1999) 123–130.

[2] M. Qamar, M. Muneer, J. Hazard. Mater. 120 (2005) 219–227.

[3] M.A. Aramendra, A. Marinas, J.M. Marinas, J.M. Moreno, F.J. Urbano, Catal. Today 101 (2005) 187–193.

[4] S. Parra, J. Oliveros, C. Pulgarin, Appl. Catal. B 31 (2002) 75–85.

[5] M. Stylidi, D.I. Kondarides, X.E. Verykios, Appl. Catal. B (2004) 189–201.

[6] Y. Xu, C.H. Langford, J. Photochem. Photobiol. A: Chem. 17 (2000) 897–902.

[7] N. Serpone, P. Marathamuthu, P. Pichat, E. Pelizzetti, H. Hidaka, J. Photochem. Photobiol. 85 (1995) 247–255.

[8] Y. Bessekhouad, D. Robert, J.V. Weber, J. Photochem. Photobiol. A 163 (2004) 569–580.

[9] H. Fujii, M. Ohtaki, K. Eguchi, J. Mol. Catal. 129 (1998) 61–68.

[10] F. Kiriakidou, D.I. Kondarides, X.E. Verykios, Catal. Today 54 (1999) 119–130.

[11] L.S. Spanhel, H. Weller, A. Henglein, J. Am. Chem. Soc. 109 (1987) 6632–6635.